Carbohydrate Polymers 112 (2014) 316–324

Contents lists available at ScienceDirect

Carbohydrate Polymers

journal homepage: www.elsevier.com/locate/carbpol

Evolution of amylopectin structure in developing wheat endosperm starch

Danusha N. Kalinga[a], Eric Bertoft[b], Ian Tetlow[c], Qiang Liu[d], Rickey Y. Yada[a], Koushik Seetharaman[b,*]

[a] Department of Food Science, University of Guelph, 116, Guelph, ON N1G 2W1, Canada
[b] Food Science and Nutrition, University of Minnesota, 225, 1334 Eckles Ave, St. Paul, MN 55108, USA
[c] Department of Molecular and Cellular Biology, Science Complex, University of Guelph, Guelph, ON N1G 2W1, Canada
[d] Guelph Food Research Centre, Agriculture and Agri-Food Canada, 93 Stone Road West, Guelph, ON N1G 5C9, Canada

ARTICLE INFO

Article history:
Received 23 August 2013
Received in revised form 2 May 2014
Accepted 6 May 2014
Available online 14 May 2014

Keywords:
Wheat
Development
Endosperm
Starch
Amylopectin

ABSTRACT

In this study, starches extracted from wheat grains harvested at 7, 14, 28, and 35 days after anthesis (DAA) were used as a means of examining the molecular structure of amylopectin (AP) from developing wheat grain. Scanning electron microscopy of wheat grain cross-sections revealed the presence of endosperm at 7 DAA and contained lenticular-shaped developing large (A-type) granules. From 14 DAA onward, spherical-shaped small (B-type) granules coexisted with large granules in the endosperm. During granule development, the fine structure of AP varied with maturity in both large and small granules. Towards the end of the pre-physiological maturity stage (28 DAA), AP in small and large granules had shortest external chain length (ECL), longest internal chain length (ICL) and lowest amount of A-chains. At physiological maturity (35 DAA), these changes in ECL, ICL and amount of A-chains were reversed when compared to 28 DAA. In both large and small granules, the external AP structure was apparently more organized at physiological maturity than at pre-physiological maturity.

1. Introduction

In wheat (*Triticum aestivum* L.), starch is deposited in the endosperm for long-term storage and accounts for about 70% of the total dry weight of the grain (Hucl & Chibbar, 1996). Endosperm is formed following pollination. The deposition of starch in the endosperm begins shortly after a period of rapid cell division and expansion (Briarty, Hughes, & Evers, 1979). The deposition of starch in endosperm starts with the initiation of large (A-type) granules at about 7 DAA to 10 DAA, followed by the initiation of small (B-type) granules at about 12 DAA to 14 DAA, and then C-type small granules around 21 DAA (Bechtel, Zayas, Kaleikau, & Pomeranz, 1990; Parker, 1985). Starch deposition in endosperm occurs until maturation (Dupont & Altenbach, 2003). The size of the large granules continues to increase until maturity, whereas the size of the small B- and C-type granules remains significantly smaller than those of the large granules (Bechtel et al., 1990). Around 35 DAA, cell expansion and water accumulation stop, protein and starch deposition ceases, and the kernel begins to desiccate. At this stage, the grain attains its maximum dry weight, or physiological maturity (Dupont & Altenbach, 2003).

The main enzymes involved in endosperm starch biosynthesis are ADP–glucose pyrophosphorylase (AGPase, involved in precursor synthesis), granule-bound starch synthase I (GBSS I, amylose synthesis), starch synthases (SS, four isoforms involved in glucan chain elongation of amylopectin), starch branching enzymes (SBE, form α-1,6 branch points in amylopectin), and starch debranching enzymes (DE, trim α-1,6 branch points to form crystalline-competent structure). Recent work also implicates an isoform of SS, SSIV, in starch granule initiation (Crumpton-Taylor et al., 2013; Roldán et al., 2007; Szydlowski et al., 2009). In the endosperm, the expression of different enzyme isoforms occurs at different times. For example, in wheat SBE IIa and IIb are expressed 13 DAA to 32 DAA, whereas SBE I is not detected until 18 DAA (Morell, Blennow, Kosar-Hashemi, & Samuel, 1997). SS I is expressed in early stages (5 DAA to 10 DAA), but in later stages, a considerable amount of the enzyme is entrapped as inactive granule-associated protein (Commuri & Keeling, 2001; Peng, Hucl, & Chibbar, 2001). In addition, different biosynthetic enzymes are active on different substrates, e.g., SBE I has a higher affinity for longer chains than SBE

* Corresponding author at: Food Science and Nutrition, University of Minnesota, 225, 1334 Eckles Ave, St. Paul, MN 55108, USA. Tel.: +1 612 624 1764; fax: +1 612 625 5272.
E-mail address: kseethar@umn.edu (K. Seetharaman).

http://dx.doi.org/10.1016/j.carbpol.2014.05.008
0144-8617/

II (Takeda, Guan, & Preiss, 1993). Differences in the action pattern of starch synthesizing enzymes suggest that starches produced at different time intervals have different structures. In addition to these differences, particular enzyme isoforms, e.g. SBEIc, are specifically associated only with large granules; however, their exact role in biosynthesis is still unclear (Peng, Gao, Baga, Hucl, & Chibbar, 2000).

The dynamic nature of the structure and composition of starch granules during endosperm development is revealed by a decrease in relative crystallinity, an increase in amylose content, and changes in the average amylopectin (AP) chain length (Kulp, 1973b; Waduge, 2012; Waduge, Xu, & Seetharaman, 2010; Wei et al., 2010). In addition, variations in the structure and functionality of large and small granules have been reported: compared to small granules, large granules have higher amounts of amylose, longer AP chain lengths, and higher gelatinization and retrogradation enthalpy; provide superior baking properties; and are less digestible (Ao & Jane, 2007; Kulp, 1973a; Liu, Gu, Donner, Tetlow, & Emes, 2007; Salman et al., 2009; Vermeylen, Goderis, Reynaers, & Delcour, 2005; Waduge, 2012; Wei et al., 2010). However, knowledge about how different expression patterns and variations in the substrate specificity of the enzyme isoforms affect structural changes in starch, especially AP, is limited.

In this investigation, amylopectin extracted from developing wheat endosperm was studied in order to acquire an understanding of the evolution of the AP structure. The primary goal was to discover whether temporal variations in biosynthesis cause structural differences in AP during the development of both small and large starch granules.

2. Materials and methods

2.1. Materials

From Eastern hard red spring wheat (Hobson variety) grown in Ontario, Canada, in 2009, wheat kernels were harvested from spikes at 7, 14, 28, and 35 DAA, with a variation of ±3 days maturity within a spike (Peterson, 1965). The selected harvesting times represented the initial starch formed, the approximate onset of small granules, the major grain filling stage, and physiological maturity, respectively. Heads were tagged when 50% of the spikelets within the head were anthesised. Soon after harvesting, spikes were stored at −20 °C to prevent any enzyme activity until the starch could be extracted.

Isoamylase (glycogen 6-glucanohydrolase; EC 3.2.1.68, ~59,000 U/mg) from *Pseudomonas* sp. was purchased from Hayashibara Biochemical Laboratories, Inc. (Okayama, Japan). Pullulanase (36.3 U/mg) from *Klebsiella planticola* (amylopectin 6-glucanohydrolase; EC 3.2.1.41) and β-amylase (705 U/mg) from barley [(1,4)-α-D-glucan maltohydrolase; EC 3.2.1.2] were purchased from Megazyme (Wicklow, Ireland). Phosphorylase *a* (~25 U/mg) from rabbit muscle [(1,4)-α-D-glucan:orthophosphate α-D-glucosyltransferase; EC 2.4.1.1] was purchased from Sigma–Aldrich (Deisenhofen, Germany).

2.2. Morphology of kernels and starch granules

The morphologies of wheat kernels and starch granules were examined using scanning electron microscopy (SEM). Samples were prepared as explained by Kalinga et al. (2013), and three kernels from each maturity stage were scanned (Hitachi S-570, Hitachi High Technologies, Tokyo, Japan) at an accelerated voltage of 10 kV.

2.3. Starch extraction and granule separation

Endosperm starch was extracted from kernels using the method developed by Waduge et al. (2010). Large and small granules were separated from starch extracted from 14, 28, and 35 DAA grains as described by Waduge (2012). The effectiveness of size separation was confirmed by measuring granule size distribution with a Mastersizer 2000 using laser light scattering (Malvern Instruments, Worcestershire, UK). The purity was generally >97% on a volume basis.

2.4. Amylopectin extraction

Amylopectin (AP) was isolated following the method given by Klucinec and Thompson (1998) with minor modifications (Bertoft, Källman, Koch, Andersson, & Åman, 2011). The yields of AP varied between 45 and 64%. The purity of the AP, which generally was >95%, was measured after debranching with pullulanase and isoamylase using gel-permeation chromatography (GPC) on Sepharose CL-6B as described by Kalinga et al. (2013).

2.5. φ,β-Limit dextrin of amylopectin

φ,β-Limit dextrin (φ, β-LD) of AP was prepared by removing external AP chains with phosphorylase *a* and β-amylase according to the method described by (Bertoft, Piyachomkwan, Chatakanonda, & Sriroth, 2008), with minor modifications, as explained by Kalinga et al. (2013).

2.6. Chain length distribution of amylopectin and φ,β-limit dextrin of amylopectin

The AP and φ,β-LD of AP were debranched with isoamylase and pullulanase at pH 5.5 (Bertoft, 2007). The chain length distribution was analyzed by high-performance anion-exchange chromatography with pulsed amperometric detection (HPAEC-PAD) (Dionex ICS 3000, Sunnyvale, CA, USA) on a CarboPac PA-100 column (4 mm × 250 mm), as described elsewhere (Bertoft, 2004). The PAD signal was converted to carbohydrate content (Koch, Andersson, & Åman, 1998).

2.7. Statistical analysis

Statistical analysis was performed by SPSS 17.0 statistical software (SPSS Inc., Chicago, IL, USA). All experiments were conducted in duplicate and the mean values are reported. Data was analyzed using one-way analysis of variance (ANOVA) and Duncan's test ($p < 0.05$).

3. Results

Developing wheat grains harvested from different maturity stages were examined by SEM. Cross-sections of kernels with starch granules in the endosperm from 7, 14, 28, and 35 DAA are shown in Fig. 1. Enlargement of the endosperm (indicated as "E") and reduction in the pericarp layer ("P") was observed with increasing grain maturity. Fig. 1a and b shows that the pericarp layer (outer layer of the grains) was relatively thick at 7 DAA and 14 DAA when compared to 28 DAA and 35 DAA. Starch co-existed in the pericarp at 7 DAA and 14 DAA as shown in Fig. 1i and j, whereas at 28 DAA and 35 DAA there was no starch observed in the pericarp layer.

At 7 DAA, lenticular granules that later developed to the population of large granules (indicated by "L") were observed (Fig. 1e). When the grain matured to 14 DAA (Fig. 1f), the initiation of spherical-shaped small granules (indicated by "S") had started. Both large and small granules continued to grow in size with increasing maturity, and the granules were more densely packed in mature endosperm at 35 DAA (Fig. 1h). As confirmed by SEM pictures, grains harvested at 7 DAA exhibited only one granule population, and the starch extracted from these grains was considered

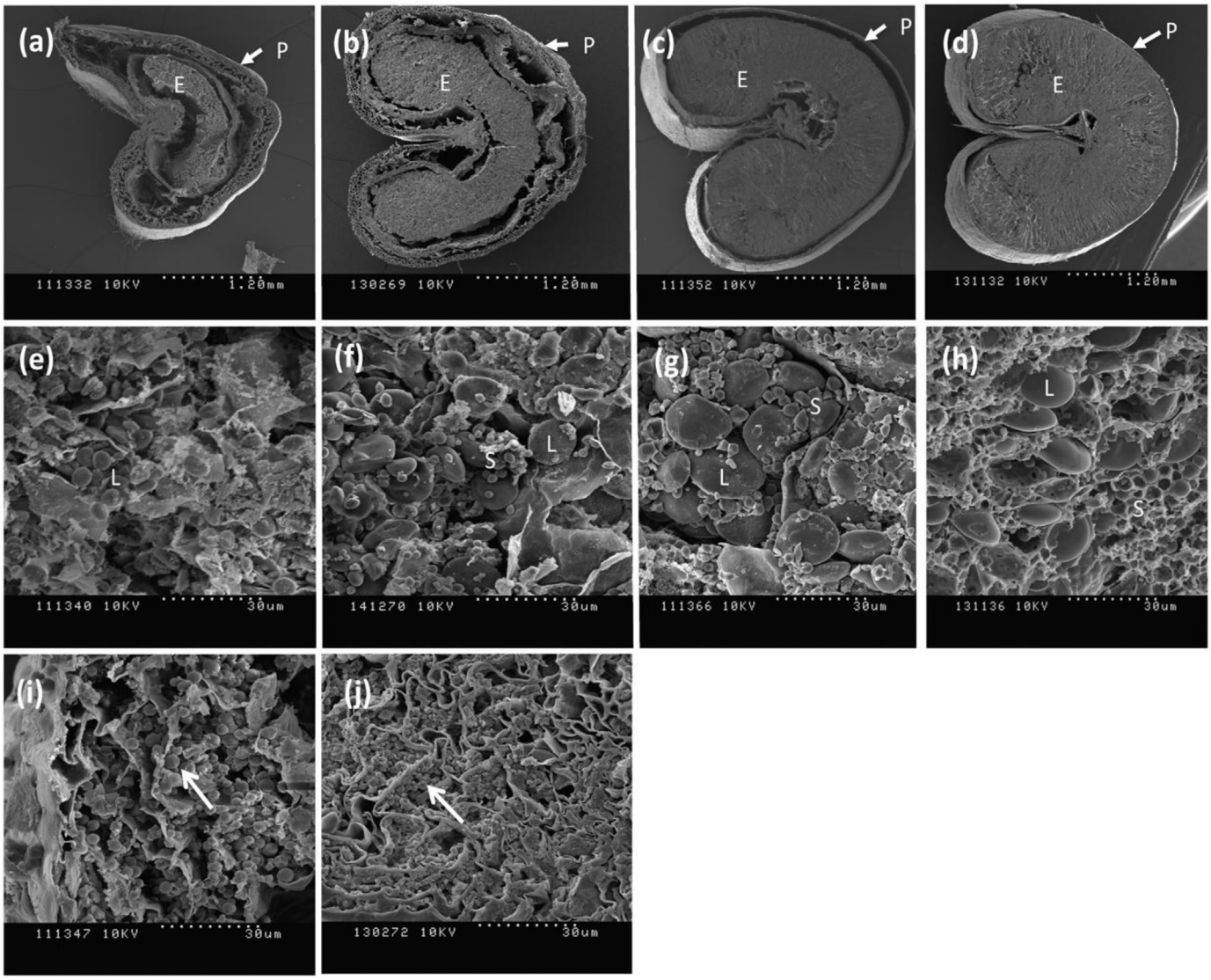

Fig. 1. Cross-sections of wheat grains harvested at different developmental stages: (a) 7 DAA; (b) 14 DAA; (c) 28 DAA; (d) 35 DAA. Starch granules at the centre of the endosperm at (e) 7 DAA with a few lenticular large starch granules; (f) 14 DAA when small spherical starch granules start to form; (g) 28 DAA; (h) 35 DAA. Starch granules in the pericarp layer of (i) 7 DAA; (j) 14 DAA; Arrows show the starch granules inside a pericarp cell; DAA = days after anthesis; E = endosperm; P = pericarp; L = large granules; S = small granules.

to be the very early stage of the development of large granules. SEM images confirmed the presence of two types of granules in grains harvested at 14, 28, and 35 DAA, and large and small granules were therefore separated from the starch extracted from these samples.

The major component of starch that determines granule organization and functionality is AP, which is a highly branched molecule, with α-1,4-linked D-glucose backbones and about 5% of α-1,6-linked branches (Pérez & Bertoft, 2010). The unit chain-length distribution of purified AP of a representative sample (from 28 DAA large granules) is shown in Fig. 2a. All preparations of AP from wheat starch granules at different growth stages had similar chain length distribution patterns, with a prominent peak at a degree of polymerization (DP) of 12, a small shoulder at DP 14, and a prominent shoulder at DP 20. The local minimum at DP 37 was used as the demarcation between long and short chains (Bertoft et al., 2008). In general, AP from large granules had slightly higher average chain lengths (CL) than AP from small granules (Table 1). At 14 DAA, however, the CL was similar in both types of granules. Later, when the CL increased in the large granules from 14 to 28 DAA, it decreased in the small granules, so that AP from 28 DAA large granules had longer average CL than AP in small granules at the same maturity. At 35 DAA, CL decreased again from 18.0 to 17.4 in the large granules, whereas CL in the small granules remained unchanged.

AP chains can be divided into internal chains and external chains. Internal chains are found between the branches in the amorphous lamellae, and external chains form the crystalline lamellae (Pérez & Bertoft, 2010). External chains were removed successively using the enzymes phosphorylase *a* and β-amylase whereby the φ,β-LD of the amylopectin was produced. In the φ,β-LD, A-chains are reduced to maltosyl stubs and, after debranching, thus give rise to a large number of chains with DP 2, with the remainder being internal B-chains. The chain length distribution of internal B-chains in φ,β-LD of a representative sample (28 DAA large) is shown in Fig. 2b. As observed with AP, φ,β-LD also exhibited a bimodal distribution of internal B-chains, with a local minimum at DP 25. Changes in the average CL of φ,β-LD (CL_{LD}) and in the internal chain length (ICL) showed a similar pattern in both types of granules (Table 1): they increased up to 28 DAA and then decreased at 35 DAA. However, with respect to large and small granules at the same maturity, no differences were apparent in either the CL_{LD} or ICL. The external

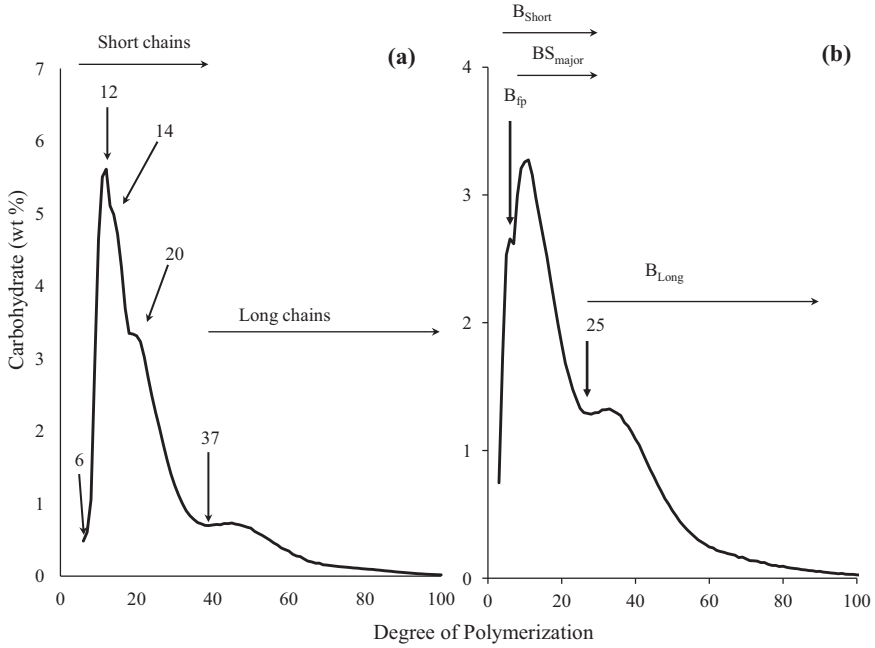

Fig. 2. Chain-length distribution of (a) wheat amylopectin from large starch granules at 28 DAA, and (b) the φ,β-limit dextrin of the same sample. Numbers represent DP (degree of polymerization); DAA = days after anthesis; short chains = DP ≤ 37; long chains = DP ≥ 38; B_{Short} (short B-chains) = DP: 3–25; B_{Long} (long B-chains) = DP ≥ 26; B_{fp} (fingerprint B-chains) = DP: 3–7; BS_{major} (major group of short B-chains) = DP: 8–25.

chain length (ECL) is the average length of the portion of the chains that is external to the branch points (Thompson, 2000). The ECL showed patterns opposite to those of the CL_{LD} or ICL (Table 1): in both large and small granules, it decreased during pre-physiological maturity (7–28 DAA) and then increased again at physiological maturity (35 DAA). Total internal chain length (TICL) is calculated by subtracting the single external glucosyl residue from the B-chains in the limit dextrins (i.e., the actual internal structure of amylopectin) (Bertoft et al., 2008). The TICL showed a pattern similar to the one observed for ICL and CL_{LD} in the large granules: an increase up to 28 DAA and then a decrease at 35 DAA. In small granules, the TICL did not change during pre-physiological maturity but decreased when the granules developed from 28 and 35 DAA (Table 1).

Relative molar amounts of different chain categories of AP and φ,β–LD are given in Table 2. A-chains do not carry any other chains on them (Peat, Whelan, & Thomas, 1956), in large granules, the number of A-chains decreased from 55.2% to 51.0% during the pre-physiological maturity period, and at the physiological maturity, it increased to 55.1% (Table 2). Similarly, in small granules, the number of A-chains decreased from 55.5% to 51.9% at pre-physiological maturity period and then increased to 56.0% at physiological maturity. The shortest A-chains are the fingerprint A-chains (A_{fp}, DP: 6–8) (Bertoft et al., 2008), which are too short to readily form double helices (Gidley & Bulpin, 1987) and are considered to be defects in the assembling of the crystalline lamellae (Koroteeva et al., 2007). The number of A_{fp}-chains, which was calculated from the AP unit chain profile, remained unchanged in the large granules during pre-physiological maturity, but they increased at 35 DAA to 6.4%. In small granules, the number of A_{fp}-chains increased especially during the pre-physiological maturity stage (5.1–6.8%). A-chains other than A_{fp}-chains were called clustered A-chains (A_{cltr}) (Bertoft et al., 2008). Changes in the number of A_{cltr}-chains were generally similar in both types of granules; i.e., during pre-physiological maturity, they decreased, and then they increased at physiological maturity (Table 2).

B-chains are chains that carry A- or B-chains, or both types of chains (Peat et al., 1956); B-chains are consequently composed of one external segment and one or several internal segments. The BS-chains (DP ≤ 25) in the φ,β-LDs of AP (Fig. 2b) were further divided into the sub-categories fingerprint B-chains (B_{fp}-chains, DP: 3–7) and the major group of short B-chains (BS_{major}-chains, DP: 8–25).

Table 1
Average chain lengths of different chain categories of amylopectin and its φ,β-limit dextrins obtained by HPAEC-PAD and the φ,β-limit value at different maturity stages of wheat ($n = 2$).

	Kernel maturity						
	Large granules				Small granules		
	7 DAA	14 DAA	28 DAA	35 DAA	14 DAA	28 DAA	35 DAA
CL_{AP}	18.2^{e}	17.6^{c}	18.0^{d}	17.4^{bc}	17.7^{c}	17.2^{ab}	17.0^{a}
CL_{LD}	7.3^{b}	7.3^{b}	8.1^{c}	6.9^{a}	7.4^{b}	7.9^{c}	6.8^{a}
ECL	12.5^{d}	11.9^{c}	11.4^{b}	11.9^{c}	11.7^{c}	10.8^{a}	11.7^{c}
ICL	4.8^{b}	4.8^{b}	5.6^{c}	4.4^{a}	4.9^{b}	5.4^{c}	4.3^{a}
TICL	12.8^{bc}	12.6^{b}	13.4^{d}	12.0^{a}	13.2^{cd}	13.3^{d}	12.0^{a}
φ,β-limit value	60.1^{c}	58.7^{bc}	55.0^{a}	60.1^{c}	57.9^{b}	53.9^{a}	59.9^{c}

Note: Values followed by a different superscript in each row are significantly different ($p < 0.05$).
DAA = days after anthesis; AP = amylopectin; CL = chain length; LD = limit dextrin; φ,β-limit value = $(CL_{AP} - CL_{LD})/CL_{AP} \times 100$; CL_{AP} = average chain length of AP; CL_{LD} = average chain length of φ,β-LD of AP; ECL (external chain length) = CL × (φ,β-limit value/100) + 1.5; ICL (internal chain length) = CL − ECL − 1; TICL = total internal chain length of B-chains.

Table 2
Relative molar concentration (%) of chain categories of amylopectin and its φ,β-limit dextrins ($n = 2$).

Chain category	Kernel maturity						
	Large				Small		
	7 DAA	14 DAA	28 DAA	35 DAA	14 DAA	28 DAA	35 DAA
A	55.2^{bc}	54.5^{b}	51.0 ^{a}	55.1^{bc}	55.5^{bc}	51.9^{a}	56.0^{c}
A_{fp}	4.8^{a}	5.3^{a}	5.4^{a}	6.4^{b}	5.1^{a}	6.8^{b}	7.1^{b}
A_{cltr}	50.4^{b}	49.2^{b}	45.7^{a}	48.7^{b}	50.4^{b}	45.1^{a}	49.0^{b}
B	44.8^{ab}	45.5^{b}	49.0^{c}	44.9^{ab}	44.5^{ab}	48.1^{c}	44.0^{a}
BS	39.0^{a}	39.8^{a}	41.8 ^{b}	39.7^{a}	38.3^{a}	41.2^{b}	39.3^{a}
B_{fp}	15.1^{a}	16.5^{d}	16.2^{cd}	17.3^{e}	14.9^{a}	15.9^{bc}	15.4^{ab}
BS_{major}	23.9^{b}	23.2^{ab}	25.6^{c}	22.3^{a}	23.4^{b}	25.3^{c}	23.9^{b}
BL	5.8^{bc}	5.8^{bc}	7.1^{d}	5.3^{b}	6.2^{c}	6.9^{d}	4.7^{a}

Note: Values followed by a different superscript in each row are significantly different ($p < 0.05$).
DP = degree of polymerization; DAA = days after anthesis; LD = limit dextrin; A-chains = DP 2 in φ,β-LD; A_{fp} (fingerprint A-chains) = DP 6–8 in whole AP; A_{cltr} (clustered A-chains) = A-chains − A_{fp}; BS (short B-chains) = DP: 3–25 in φ,β-LD; BL (long B chains) = DP ≥ 26 in φ,β-LD; B_{fp} (fingerprint B-chains) = DP: 3–7 in φ,β-LD; BS_{major} (major group of short B-chains) = DP: 8–25 in φ,β-LD.

Changes in the number of B_{fp}-chains possessed different patterns in large and small granules (Table 2). In large granules, the number of B_{fp}-chains increased throughout maturity, with the largest number appearing at 35 DAA (17.3%). In small granules, however, the number of B_{fp}-chains increased until 28 DAA and then remained constant until physiological maturity. Both large and small granules exhibited the greatest number of BS_{major}-chains at 28 DAA. B-chains longer than DP 26 in the φ,β-LDs are considered to be long B-chains (BL). The pattern of change in the number of BL-chains during granule development was similar to that for BS_{major}-chains.

4. Discussion

This investigation presents evidence for changes in the morphology and molecular structure of starch from developing wheat endosperm. In accordance with previous findings (Bechtel et al., 1990), enlargement of the endosperm, and the initiation of lenticular-shaped large granules, followed by the initiation of spherical-shaped small granules, were evident in scanning electron micrographs (Fig. 1). Previous work conducted on the same material (Eastern hard red winter wheat, variety Hobson) also showed changes in the size distribution of developing wheat endosperm starches (Waduge, 2012). According to the findings in that study, both small and large granules increased in size throughout the maturity unit 35 DAA, after which there was no increase in size indicating that there was no growth of starch granules after physiological maturity. At 7 DAA, grains had one size-population of starch granules (~1–15 μm), but from 14 DAA onward, two populations with two distinct sizes were found. The size of large granules increased to ~45 μm when the granules had developed to 35 DAA. In contrast, the size of the small granules did not change dramatically with maturity, and their size ranged between 1 and 10 μm at 35 DAA (Waduge, 2012).

At 7 and 14 DAA pericarp starch co-existed with endosperm starch (Fig. 1i and j). The diameter of the pericarp starch granules ranged from 1 to 6 μm (Kalinga et al., 2013). Visual evidence therefore indicated that some pericarp starch contamination was expected in the preparations of 7 DAA large starch granules and in 14 DAA small starch granules.

4.1. Development of amylopectin structure at pre-maturity stage

This investigation considered the structural development of AP through pre-physiological maturity up to physiological maturity at 35 DAA. The AP structure of both small and large granules changed continuously during this time (Tables 1 and 2). Waduge et al. (2010) studied granular starch from developing wheat endosperm and found that starch harvested at 28 DAA had longer chains that can bind with iodine. The results of the current study showed that both types of granules had longer ICL and TICL and more BL-chains at 28 DAA than at other maturity stages. In addition to the structural changes in AP during granule development, differences were apparent between large and small granules throughout all development stages. In general, large granules had more BL-chains than small granules (Table 2). This has also been previously observed in large and small granules from barley, triticale and wheat (Ao & Jane, 2007; Salman et al., 2009). However, the specific reason for the structural differences in AP of large and small granules are as yet unknown.

The expression pattern and substrate affinity of the biosynthetic enzymes could be considered as the primary reasons for the time-dependent structural changes in AP. It has been demonstrated that phosphorylation-dependent complexes exist between SBE and SS isoforms (Tetlow et al., 2004). In wheat protein, complexes are formed around 10 to 15 DAA; prior to this development stage, SSI, SS II, and SBE II are present in wheat endosperm in monomeric form (Tetlow et al., 2008). In wheat endosperm, SS I expression is high around 5 to 10 DAA (Peng et al., 2001). When glucan chains reach a critical length, they become unsuitable for catalysis by SS I, which may then become entrapped inside the granules as a relatively inactive protein (Commuri & Keeling, 2001). The short chains produced by SS I are elongated by SS IIa and SS IIIa (Commuri & Keeling, 2001). These new long chains provide sufficient substrates for the activity of SBE IIa and IIb (Morell et al., 1997). SBE II forms branches preferentially by cutting segments from the most abundant chain categories (DP > 12) and adding them to shorter chains (DP: 6–11) (Nielsen, Baunsgaard, & Blennow, 2002) and has recently been shown, in vitro, to catalyze the branching reaction after chain elongation by SSIIa when the proteins are associated in a complex (Liu et al., 2012).

The changes that occur in the AP structure during the pre-physiological maturity in both large and small granules are modelled in Fig. 3. The models suggest possible modes of SBE action that could produce the differences detected in the chain lengths and in the proportions of chain categories (Tables 1 and 2). The net effects of alternative chain transfer reactions are compared with the experimental observations. Fig. 3a depicts the possible structural changes that result from the transfer by SBE II of a segment of an A-chain to an existing B_{fp}-chain. According to this model, the number of B_{fp}-chains decreases because the B_{fp}-chain is converted into a BS_{major}-chain. Therefore, BS_{major}-chains and A-chains increase in number and internal segments (TICL and ICL) increase in length. After the SBE II action, SSs are thought to further elongate the external parts of the chains so that the net effect on the ECL becomes negligible. The theoretical increase in BS_{major}-chains agrees with the experimentally found increase; however, the experimental data

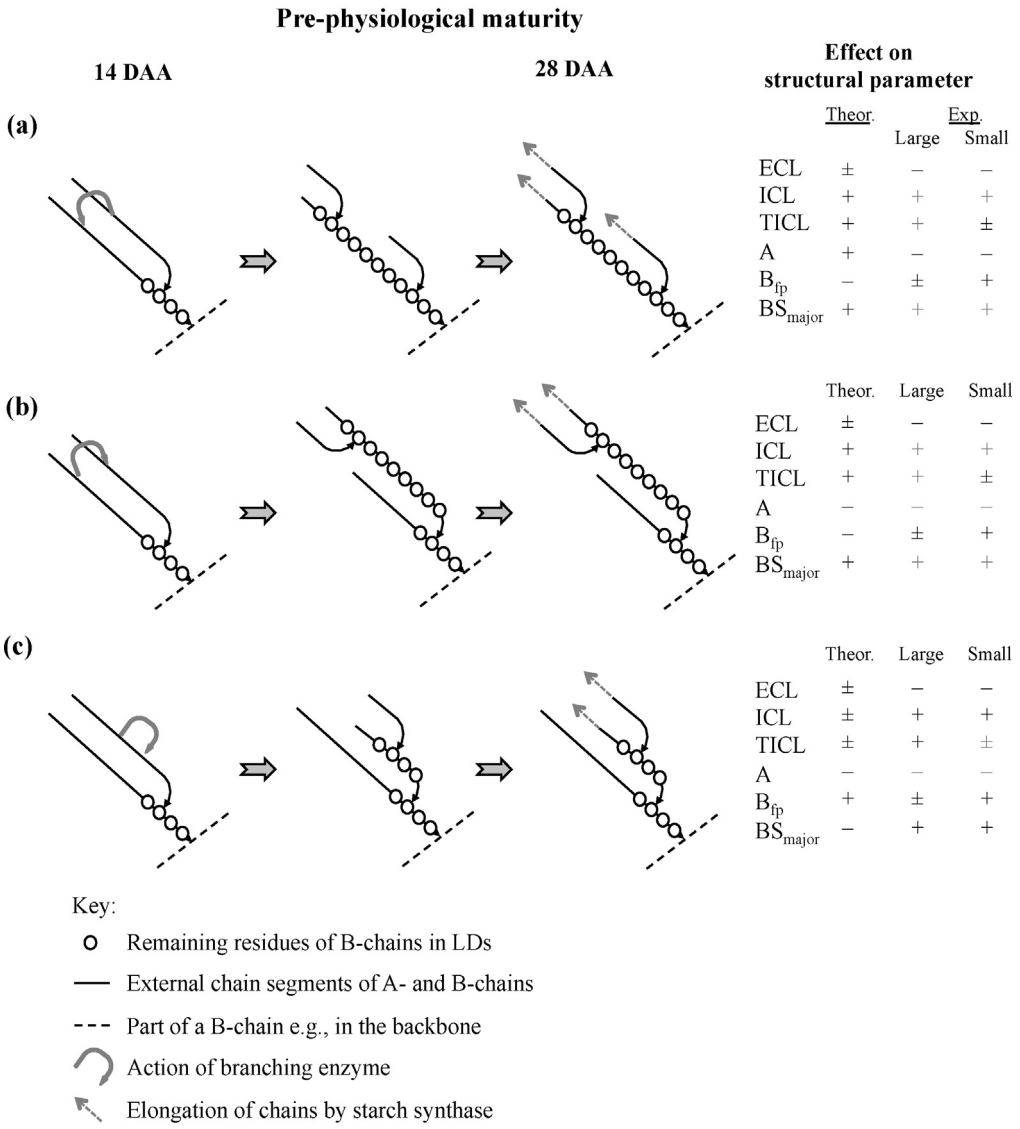

Fig. 3. Possible models for structural changes in wheat endosperm AP during pre-physiological maturity: (a) SBE II catalyses transfer from an A-chain to an existing B_{fp}-chain; (b) SBE II catalyses transfer from an external B-chain to an A-chain forming a new BS_{major}-chain; (c) SBE II catalyses transfer from an A-chain to the same A-chain, forming a new BS_{major}-chain. Theoretical positive (+), negative (−), and neutral (±) effects on the structural parameters are indicated and compared with the actual experimentally detected changes in large and small granules. SBE II = branching enzyme II; B_{fp} = fingerprint B-chains; BS_{major} = major group of short B-chains.

do not correspond to the theoretically predicted effects on A- and B_{fp}-chains. It, therefore, appears that this mode of SBE action is not the only mechanism of chain transfer. Fig. 3b depicts possible changes that occur when SBE II transfers an external B-chain segment to the non-reducing end-side of an A-chain. This mode of action converts the A-chain into a BS_{major}-chain, with a theoretically predictable increase in the number of BS_{major}-chains and a decrease in B_{fp}-chains; as a consequence, the relative number of A-chains is reduced and, as shown in Fig. 3b, the length of the internal segments (ICL) increases. With the exception of the decrease in the number of B_{fp}-chains, this mode of SBE action agrees fairly well with the experimental results, especially for large granules. As shown in Fig. 3c, SBE II transfers a segment of an A-chain back to the same A-chain (or alternatively to another A-chain), this time close to the reducing-end side. According to this model, the initial A-chain is converted to a B_{fp}-chain, increasing the relative number of B_{fp}-chains and decreasing that of the A-chains; in addition, the TICL and ICL are unchanged because there is no effect on the length of the internal segments. This explanation fits rather well with the changes observed in the small granules, i.e., no significant differences in the TICL were found. Additional deductions can be made with respect to chain transfers, but it is apparent that any single type of chain transfer cannot explain all of the changes that occur during AP biosynthesis.

4.2. Mature amylopectin structure

When a wheat grain reaches its physiological maturity (around 35 DAA), it has no supply of sugars, proteins, or water. At this time, the endosperm tissue undergoes a form of apoptosis, and the grain begins to desiccate (Dupont & Altenbach, 2003). Noticeably, the structural changes that were observed at physiological maturity occurred primarily in reverse order compared to the changes during the pre-physiological maturity up to 28 DAA. In addition to the SBE II expressed during the early maturity stages, the expression of SBE I starts after 18 DAA (Morell et al., 1997); the expression

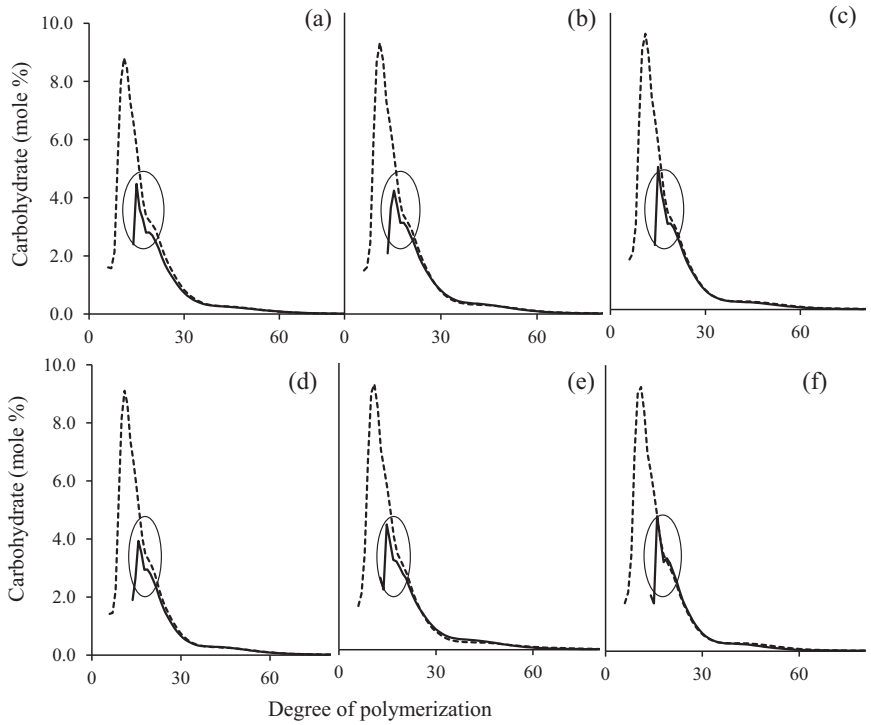

Fig. 4. Reconstruction of the molar distribution B-chains (—) from the distribution of φ,β-LD of amylopectin from developing wheat endosperm. The profiles are compared with the experimentally obtained distribution of chains in parent amylopectin (- -). The encircled area in each graph indicate areas with variable good or poor matching of theoretical values with experimental values: (a) 14 DAA large granules; (b) 28 DAA large granules; (c) 35 DAA large granules; (d) 14 DAA small granules; (e) 28 DAA small granules; (f) 35 DAA small granules. DAA = days after anthesis; φ,β-LD = φ,β limit dextrin.

level of SBE I is greater than that of SBE II at about 28 DAA (Shewry et al., 2009). The protein complexes that are formed with SBE I and SS (mainly SS III) are believed to be involved in the synthesis of the BL-chains that are present in amorphous lamellae (Tetlow, 2011). At 28 DAA, both large and small granules had the longest ICL and the greatest number of BL-chains. In line with the views of some researchers (Nakamura, 2002; Tetlow, 2011), the current study shows the reduction at 35 DAA of ICL and TICL (Table 1) and amount of BL-chains (Table 2).

The reason for the increase in the ECL at 35 DAA is unclear. However, a possible cause could be glucan trimming by debranching enzymes (DE). Throughout the starch biosynthetic process, DE play a critical role in forming the amylopectin structure (Ball et al., 1996; Nakamura, 2002) and, apparently, this could also be a reason for the other structural changes observed. Within this context, it is of interest to consider the connection between the unit chain profile of the amylopectin and its limit dextrin. As in the φ,β-LD the external chains have been removed, it is possible to theoretically reconstruct the original positions of the B-chains in the unit chain profile by adding the external segments back to the B-chains. In practice, however, since the exact external length for each individual chain is unknown, the average ECL value can be used and added to the profile of B-chains. Such reconstructions have shown that the theoretically constructed curves of B-chains generally are in good agreement with experimentally measured profiles (Bertoft, 2004; Bertoft & Koch, 2000; Bertoft et al., 2008).

Fig. 4 illustrates reconstructions of the molar distribution of the B-chains and provides a comparison with the experimental profiles of the unit chains of the original AP. For DP > 16, the theoretical profiles of the B-chains were in good agreement with the experimental unit chain profiles of AP from fully matured large and small granules (35 DAA), suggesting that B-chains in this DP-range carry external chains that correspond closely to the average ECL. This result was, thus, in general agreement with findings for many other starches and suggested a well-ordered external structure. However, at the pre-physiological maturity stages the reconstructed B-chains profiles were in poor agreement with the experimental curves for DP up to the order of 25 or 30. This discrepancy suggested that the length of the external B-chain segments differed significantly from the average ECL value; it also implied a comparatively broad overlapping area of A- and B-chains. It appeared, therefore, that the external structure of the amylopectin components was more irregular during the pre-physiological maturity stage with large variations in external chain lengths; and glucan trimming might result in a more even structure suitable for crystallization.

Fig. 5 shows possible modes of glucan trimming at physiological maturity. Fig. 5a depicts possible changes in the structure when DE removes an A-chain attached to a B_{fp}-chain, which results in increased ECL and a larger number of A-chains. The number of B_{fp}-chains drops and the number of BS_{major}-chains remains unchanged. Experimentally, however, the latter chain category decreased in number (Table 2). Fig. 5b illustrates a possible explanation of the changes that might be expected when DE removes an A-chain that is attached to a BS_{major}-chain. This also increases ECL and the number of A-chains. However, this model fails to include changes in the B_{fp}-chains. Fig. 5c provides an explanation of the changes that might occur when a BS_{major}-chain accommodates multiple A-chains, some of which are removed by DE. In this model, both the ECL and the number of B_{fp}-chains increase, whereas BS_{major}-chains decrease. However, the number of A-chains also decreases, which is in disagreement with the experimental finding. Again, therefore, if glucan trimming is the major reason for the changes in amylopectin structure at the late stage of wheat starch development, any one of the mechanisms proposed in Fig. 5 is apparently insufficient to explain the evolving structure found experimentally.

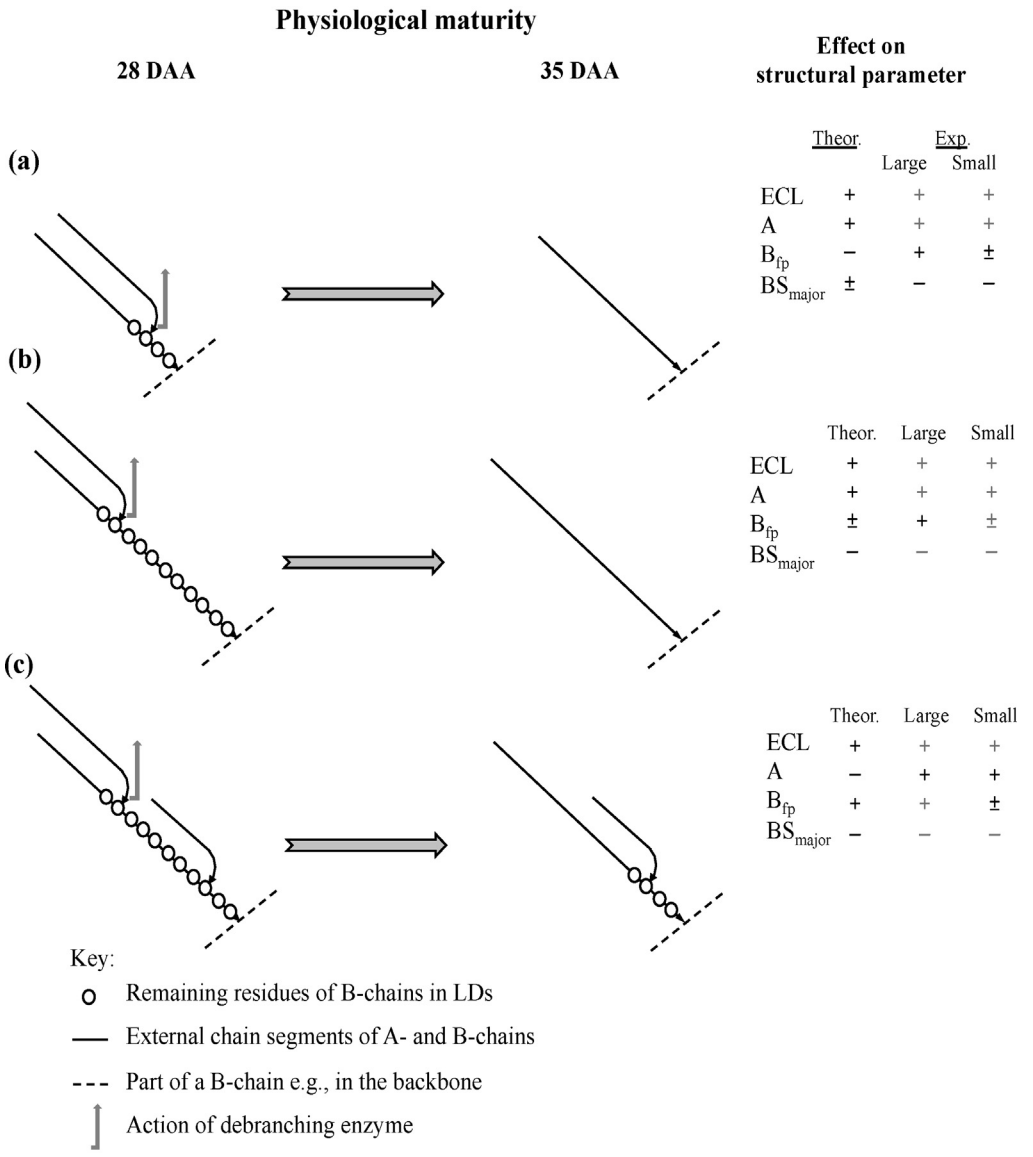

Fig. 5. Possible models for glucan trimming in wheat endosperm AP at physiological maturity: (a) DE removes an A-chain attached to a B_{fp}-chain; (b) DE removes an A-chain attached to a BS_{major}-chain; (c) a BS_{major}-chain accommodates multiple A-chains, some of which are removed by DE. Theoretical positive (+), negative (−), and neutral (±) effects on the structural parameters are indicated and compared with the actual experimentally detected changes in large and small granules. DE = debranching enzyme; B_{fp} = fingerprint B-chains; BS_{major} = major group of short B-chains.

5. Conclusion

In developing wheat endosperm, only large granules are visible at 7 DAA. From 14 DAA onwards, small granules exist with large granules. The AP structure changes continuously until physiological maturity. Both large and small granules undergo similar changes during pre-physiological maturity, showing a decrease in the number of A-chains and an increase in the number of B_{fp}-, BS_{major}-, and BL-chains. During this period, the average CL and ECL of AP decreases, but ICL increases. At physiological maturity ECL is again higher in both types of granules, and both types of granules appear to have a more organized AP structure than at pre-physiological maturity. When granules develop from the end of the pre-physiological maturity stage, internal BL- and BS_{major}-chains appear to act as donor chains for branching. The new chains produced in small and large granules are mostly A- and B_{fp}-chains. Thus, both the external and internal structure of AP changes throughout endosperm development.

Acknowledgement

We greatly appreciate the efforts of Mr. Mark Etienne, of Dow AgroSciences, who assisted with sampling wheat in the field.

References

Ao, Z., & Jane, J.-l. (2007). Characterization and modeling of the A- and B-granule starches of wheat, triticale, and barley. *Carbohydrate Polymers*, *67*, 46–55.
Ball, S., Guan, H. P., James, M., Myers, A., Keeling, P., Mouille, G., et al. (1996). From glycogen to amylopectin: a model for the biogenesis of the plant starch granule. *Cell*, *86*, 349–352.
Bechtel, D. B., Zayas, I., Kaleikau, L., & Pomeranz, Y. (1990). Size-distribution of wheat starch granules during endosperm development. *Cereal Chemistry*, *67*, 59–63.
Bertoft, E. (2004). On the nature of categories of chains in amylopectin and their connection to the super helix model. *Carbohydrate Polymers*, *57*, 211–224.
Bertoft, E. (2007). Composition of building blocks in clusters from potato amylopectin. *Carbohydrate Polymers*, *70*, 123–136.
Bertoft, E., Källman, A., Koch, K., Andersson, R., & Åman, P. (2011). The cluster structure of barley amylopectins of different genetic backgrounds. *International Journal of Biological Macromolecules*, *49*, 441–453.

Bertoft, E., & Koch, K. (2000). Composition of chains in waxy-rice starch and its structural units. *Carbohydrate Polymers*, *41*, 121–132.
Bertoft, E., Piyachomkwan, K., Chatakanonda, P., & Sriroth, K. (2008). Internal unit chain composition in amylopectins. *Carbohydrate Polymers*, *74*, 527–543.
Briarty, L. G., Hughes, C. E., & Evers, A. D. (1979). The developing endosperm of wheat – a stereological analysis. *Annals of Botany*, *44*, 641–658.
Commuri, P. D., & Keeling, P. L. (2001). Chain-length specificities of maize starch synthase I enzyme: Studies of glucan affinity and catalytic properties. *The Plant Journal*, *25*, 475–486.
Crumpton-Taylor, M., Pike, M., Lu, K.-J., Hylton, C. M., Feil, R., Eicke, S., et al. (2013). Starch synthase 4 is essential for coordination of starch granule formation with chloroplast division during Arabidopsis leaf expansion. *New Phytologist*, *200*, 1064–1075. http://dx.doi.org/10.1111/nph.12455
Dupont, F. M., & Altenbach, S. B. (2003). Molecular and biochemical impacts of environmental factors on wheat grain development and protein synthesis. *Journal of Cereal Science*, *38*, 133–146.
Gidley, M. J., & Bulpin, P. V. (1987). Crystallisation of malto-oligosaccharides as models of the crystalline forms of starch: Minimum chain-length requirement for the formation of double helices. *Carbohydrate Research*, *161*, 291–300.
Hucl, P., & Chibbar, R. N. (1996). Variation for starch concentration in spring wheat and Its repeatability relative to protei concentration. *Cereal Chemistry*, *73*, 756–758.
Kalinga, D. N., Waduge, R., Liu, Q., Yada, R. Y., Bertoft, E., & Seetharaman, K. (2013). On the differences in the granular architecture and starch structure between pericarp and endosperm wheat starches. *Starch/Stärke*, *65*, 791–800.
Klucinec, J. D., & Thompson, D. B. (1998). Fractionation of high-amylose maize starches by differential alcohol precipitation and chromatography of the fractions. *Cereal Chemistry*, *75*, 887–896.
Koch, K., Andersson, R., & Åman, P. (1998). Quantitative analysis of amylopectin unit chains by means of high-performance anion-exchange chromatography with pulsed amperometric detection. *Journal of Chromatography A*, *800*, 199–206.
Koroteeva, D. A., Kiseleva, V. I., Sriroth, K., Piyachomkwan, K., Bertoft, E., Yuryev, P. V., et al. (2007). Structural and thermodynamic properties of rice starches with different genetic background: Part 1. Differentiation of amylopectin and amylose defects. *International Journal of Biological Macromolecules*, *41*, 391–403.
Kulp, K. (1973a). Characteristics of small-granule starch of flour and wheat. *Cereal Chemistry*, *50*, 666–679.
Kulp, K. (1973b). Some properties of starches derived from wheat of varied maturity. *Cereal Chemistry*, *50*, 498–504.
Liu, F., Romanova, N., Lee, E. A., Ahmed, R., Evans, M., Gilbert, E. P., et al. (2012). Glucan affinity of starch synthase IIa determines binding of starch synthase I and starch branching enzyme IIb to starch granules. *Biochemical Journal*, *448*, 373–387.
Liu, Q., Gu, Z., Donner, E., Tetlow, I., & Emes, M. (2007). Investigation of digestibility in vitro and physicochemical properties of A- and B-type starch from soft and hard wheat flour. *Cereal Chemistry*, *84*, 15–21.
Morell, M. K., Blennow, A., Kosar-Hashemi, B., & Samuel, M. S. (1997). Differential expression and properties of starch branching enzyme isoforms in developing wheat endosperm. *Plant Physiology*, *113*, 201–208.
Nakamura, Y. (2002). Towards a better understanding of the metabolic system for amylopectin biosynthesis in plants: rice endosperm as a model tissue. *Plant and Cell Physiology*, *43*, 718–725.
Nielsen, T. H., Baunsgaard, L., & Blennow, A. (2002). Intermediary glucan structures formed during starch granule biosynthesis are enriched in short side chains, a dynamic pulse labeling approach. *Journal of Biological Chemistry*, *277*, 20249–20255.
Parker, M. L. (1985). The relationship between A-type and B-type starch granules in the developing endosperm of wheat. *Journal of Cereal Science*, *3*, 271–278.
Peat, S., Whelan, W. J., & Thomas, G. J. (1956). The enzymic synthesis and degradation of starch. Part XXII. Evidence of multiple branching in waxy-maize starch. A correction. *Journal of the Chemical Society*, 3025–3030.
Peng, M., Gao, M., Baga, M., Hucl, P., & Chibbar, R. N. (2000). Starch-branching enzymes preferentially associated with A-type starch granules in wheat endosperm. *Plant Physiology*, *124*, 265–272.
Peng, M., Hucl, P., & Chibbar, R. N. (2001). Isolation, characterization and expression analysis of starch synthase I from wheat (*Triticum aestivum* L.). *Plant Science*, *161*, 1055–1062.
Pérez, S., & Bertoft, E. (2010). The molecular structures of starch components and their contribution to the architecture of starch granules: A comprehensive review. *Starch/Stärke*, *62*, 389–420.
Peterson, R. F. (1965). *Wheat: Botany, cultivation, and utilization*. New York: Interscience Publisher Inc.
Roldán, I., Lucas, M. M., Delvallé, D., Planchot, V., Jimenez, S., Perez, R., et al. (2007). The phenotype of soluble starch synthase IV defective mutants of *Arabidopsis thaliana* suggests a novel function of elongation enzymes in the control of starch granule formation. *Plant Journal*, *49*, 492–504.
Salman, H., Blazek, J., Lopez-Rubio, A., Gilbert, E. P., Hanley, T., & Copeland, L. (2009). Structure-function relationships in A and B granules from wheat starches of similar amylose content. *Carbohydrate Polymers*, *75*, 420–427.
Shewry, P. R., Underwood, C., Wan, Y., Lovegrove, A., Bhandari, D., Toole, G., et al. (2009). Storage product synthesis and accumulation in developing grains of wheat. *Journal of Cereal Science*, *50*, 106–112.
Szydlowski, N., Ragel, P., Raynaud, S., Lucas, M. M., Roldán, I., Montero, M., et al. (2009). Starch granule initiation in *Arabidopsis* requires the presence of either class IV or class III starch synthases. *Plant Cell*, *21*, 2443–2457.
Takeda, Y., Guan, H.-P., & Preiss, J. (1993). Branching of amylose by the branching isoenzymes of maize endosperm. *Carbohydrate Research*, *240*, 253–263.
Tetlow, I. (2011). Starch biosynthesis in developing seeds. *Seed Science Research*, *21*, 5–32.
Tetlow, I. J., Beisel, K. G., Cameron, S., Makhmoudova, A., Liu, F., Bresolin, N. S., et al. (2008). Analysis of protein complexes in wheat amyloplasts reveals functional interactions among starch biosynthetic enzymes. *Plant Physiology*, *146*, 1878–1891.
Tetlow, I. J., Wait, R., Lu, Z., Akkasaeng, R., Bowsher, C. G., Esposito, S., et al. (2004). Protein phosphorylation in amyloplasts regulates starch branching enzyme activity and protein–protein interactions. *The Plant Cell*, *16*, 694–708.
Thompson, D. B. (2000). On the non-random nature of amylopectin branching. *Carbohydrate Polymers*, *43*, 223–239.
Vermeylen, R., Goderis, B., Reynaers, H., & Delcour, J. A. (2005). Gelatinisation related structural aspects of small and large wheat starch granules. *Carbohydrate Polymers*, *62*, 170–181.
Waduge, R. (2012). Morphology and molecular organization of developing wheat starch granules. In *Food science* (PhD Thesis). Guelph: University of Guelph., p. 308.
Waduge, R. N., Xu, S., & Seetharaman, K. (2010). Iodine absorption properties and its effect on the crystallinity of developing wheat starch granules. *Carbohydrate Polymers*, *82*, 786–794.
Wei, C., Zhang, J., Chen, Y., Zhou, W., Xu, B., Wang, Y., et al. (2010). Physicochemical properties and development of wheat large and small starch granules during endosperm development. *Acta Physiologiae Plantarum*, *32*, 905–916.